

A Virus Aerosol Chamber Study: The Impact of UVA, UVC, and H₂O₂ on Airborne Viral Transmission

Ali Mohamadi Nasrabadi, Diana Eckstein, Peter Mettke, Nawras Ghanem, René Kallies, Matthias Schmidt, Falk Mothes, Thomas Schaefer, Ricarda Graefe, Chaturanga D. Bandara, Melanie Maier, Uwe Gerd Liebert, Hans Richnow, and Hartmut Herrmann*

Cite This: *Environ. Health* 2025, 3, 648–658

Read Online

ACCESS |

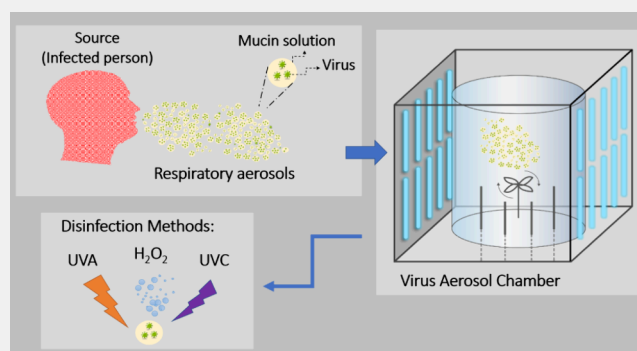
Metrics & More

Article Recommendations

Supporting Information

ABSTRACT: The COVID-19 pandemic highlighted the urgent need to control airborne virus transmission, particularly in indoor environments with limited ventilation. This study evaluates the effectiveness of UVA and UVC irradiation, along with hydrogen peroxide (H₂O₂), in inactivating aerosolized viruses. A 19 m³ virus aerosol simulation chamber, replicating indoor conditions, was used to simulate human respiratory emissions by aerosolizing *Escherichia* phage T4 (T4 phages) embedded in a pig mucin medium that mimics respiratory aerosols. Results showed a clear, dose-dependent reduction in viral genome copies with UVC exposure, where a dose of 129.9 mJ/cm² reduced over 99% of the viral genome copies. Although less efficient, UVA still contributed to virus inactivation, reducing detectable phages to 20% at 513.30 J/cm². Mucin provided a protective effect, making virus removal more challenging. Hydrogen peroxide enhanced disinfection, with 1.6 ppm reducing viral genome copies by 78%, and higher concentrations (up to 16 ppm) achieving over 99% reduction in the dark condition. The combination of UVA/UVC with H₂O₂ further enhanced disinfection, eliminating detectable virus genome copies entirely. These findings underscore the potential for using combined UV light and chemical treatments to effectively mitigate airborne viral transmission in enclosed spaces.

KEYWORDS: Aerosolized Virus Transmission, Mucin, UVA, UVC, Hydrogen Peroxide (H₂O₂), Virus Aerosol Chamber, Quantitative PCR (qPCR)



INTRODUCTION

Data of the World Health Organization (WHO)¹ reveal that by June 2024, nearly 800 million COVID-19 cases and approximately 7 million deaths were reported globally. Notably, survivors may suffer significant long-term sequelae including respiratory, cardiac, and psychological disorders, with a heightened risk of early mortality.² Ahmed et al.² found that around one-third of survivors endured long-term severe or critical conditions. For COVID-19, similar patterns emerge, with up to a quarter of patients experiencing lasting impairments from severe illness, such as acute respiratory distress syndrome (ARDS), chronic lung damage, cardiovascular complications, and persistent fatigue. These complications often result in reduced physical functioning and health-related quality of life (HRQoL), as well as mental health challenges like anxiety and depression in many patients postrecovery.³ Beyond direct health impacts, the pandemic has taken a heavy economic toll, evident in widespread industry shutdowns, quarantine measures, and increased layoffs. Cutler and Summers⁴ estimated that, by the fall of 2021, the economic impact in the United States alone, when

considering reductions in economic output and health, exceeded \$16 trillion, approximately equal to 90% of the yearly United States GDP (Gross Domestic Product).

The primary transmission route for Severe Acute Respiratory Syndrome Coronavirus 2 (SARS-CoV-2), the virus responsible for COVID-19, is through respiratory droplets and aerosols emitted during exhalation.^{4–8} The American Center for Disease Control and Prevention (CDC) identified inhalation of fine respiratory droplets and aerosol particles as a major exposure pathway of SARS-CoV-2.⁹ Previous laboratory studies have shown that SARS-CoV-2 remains viable in aerosol particles over several hours. Aerosol transmission has been found to be influenced by factors such as size distribution

Received: October 14, 2024

Revised: January 28, 2025

Accepted: February 1, 2025

Published: March 7, 2025



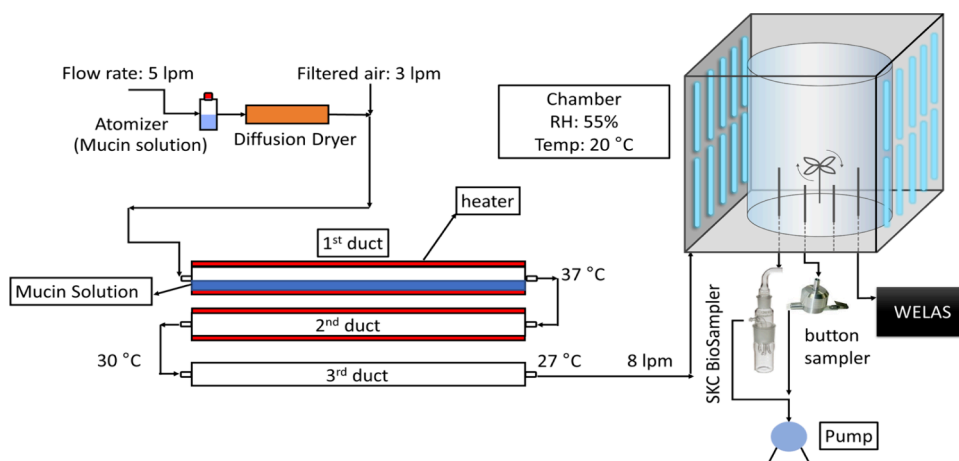


Figure 1. Experimental schematic setup to evaluate the effect of UV and H_2O_2 on aerosolized virus inside the atmospheric chamber.

(influenced by physical activity, gender, and intensity of lip movements of tested humans¹⁰) and environmental conditions, including temperature (T), relative humidity (RH), atmospheric particulate matter (PM), air flow speed and direction, and lighting conditions.¹¹ To combat the virus, strategies such as vaccination, mask-wearing, testing, contact tracing, and social distancing were implemented.¹² Despite their effectiveness, these measures led to disruptions in daily life, economic challenges, and strains on healthcare systems, highlighting the need for efficient pandemic management solutions.^{13,14} Traditional air ventilation strategies, while beneficial, have limitations in energy efficiency and hygiene, especially during the colder months with their higher viral infection rates. This has spurred the development and application of air decontamination technologies.¹²

Within the present study, virus transmission through aerosol particles, often referred to as the “airborne route”, was simulated using controlled chamber experiments. To achieve this, we upgraded an existing facility to a virus aerosol simulation chamber. This setup allows for the characterization of different loss processes and deactivation pathways of virus-loaded aerosols, enabling us to fully describe them physico-chemically. This approach helps to identify the most promising strategies for reducing the viral load within these aerosol particles, thus mitigating the potential for virus transmission through the air. With the present study, the effects of UV deactivation and the influences of H_2O_2 on T4 phages were investigated.

UV irradiation is a well-established method for inactivating bioaerosols including viruses, bacteria, and fungi.¹⁵ Because of its short wavelength (100–280 nm) and high energy, UVC radiation irreversibly interacts with and destroys the viral genome when it penetrates into viral particles. The primary effect of UVC is the deformation of nucleic acids, leading to the formation of pyrimidine dimers that disrupt DNA’s double-helix structure. This alteration impedes proper transcription and replication of RNA and DNA, effectively halting cellular replication and resulting in viral inactivation.^{16,17} Literature suggests that UVC doses required for inactivating 99.9% of viruses range between 1 and 2 mJ/cm^2 .^{18–21} Tseng and Li¹⁹ reported the effect of UVC on inactivation of different kinds of bacteriophages. Although the type of virus is important, as different viruses require different UVC doses for inactivation, the necessary radiation dose is also influenced by the carrier medium, which can alter how UVC radiation interacts with the

virus and its environment. For example, UVC effectiveness can be reduced in turbid or protective mediums like mucin.^{22–24} In contrast to the short wavelength UVC ($180 \text{ nm} \leq \lambda \leq 280 \text{ nm}$), UVA light has a longer wavelength range (320–400 nm) and lower energy, limiting its penetration and direct genomic impact.^{25,26} However, UVA directly damages various components, including nucleic acids, proteins, and membranes. Although UVA is effective for disinfection, its lower efficiency requires higher energy doses. To overcome this, nanoparticles such as TiO_2 and CuO are at times employed as photocatalysts to generate reactive oxygen species (ROS) which could inactivate airborne viruses upon exposure to UVA light.^{27,28}

Hydrogen peroxide (H_2O_2) is a well-known disinfectant for surfaces to remove pathogen contaminations like viruses, bacteria, fungi, and spores. H_2O_2 inactivates viruses by oxidizing critical components, such as lipid membranes and nucleic acids. The O–O bond in H_2O_2 can be easily cleaved thermally or photochemically to yield hydroxyl radicals ($\cdot\text{OH}$) which very efficiently damage the aforementioned biological components of the viruses, effectively leading to their deactivation.²⁹ While most studies focus on surface disinfection,³⁰ the role of H_2O_2 in air sanitization has gained attention only recently. Gomez et al.³¹ investigated the effect of H_2O_2 on aerosolized murine coronavirus in a 9 m^3 chamber under dark conditions. Their results demonstrated that 99% of the virus was removed under dark conditions. However, apparently, further studies are necessary to evaluate the efficacy of H_2O_2 at different concentrations, in conjunction with UV exposure for different wavelengths and intensities and in various environments.

Within the present study, an experimental setup was designed to produce aerosolized virus particles that closely simulate human breath exhaust particles. To create a realistic environment, a complex mixture of deionized water, pig mucin, lipid, and salt was used as an aerosol carrier solution. In control experiments, virus viability in the thus generated particles of complex composition was compared with that when particles solely consisted of deionized water. After generation, particles were introduced into an aerosol simulation chamber with a volume of 19 m^3 . The research aim was to provide a comprehensive assessment of the environmental factors influencing virus viability and the potential of irradiation for removing airborne viruses. The effect of UVA and UVC radiation at varying light intensities and exposure times was investigated using a T4 phage. Furthermore, the disinfection

potential of gas phase hydrogen peroxide at different concentrations, both in the absence of light and under exposure to varying levels of UVA and UVC radiation for different durations, was explored.

METHODS AND MATERIAL

Experimental Setup: Particle Generation, Virus Addition, and Chemical Composition Matching to Human Exhalation Aerosol

The experimental setup consists of an aerosol generator, an atmospheric chamber, and two biosamplers (Figure 1). A homemade atomizer (comparable to an atomizer available from TSI, Model 3076) was used to generate aerosolized particles. Ammonium sulfate (Sigma-Aldrich, 99.99% purity) was used as a replacement for the virus particles for initial setup verification and size measurements. In the virus runs, T4 phage was used and added to the seed solution.

The mucin solution used to simulate human respiratory droplets containing viruses, consisted of NaCl (9 g/L), porcine gastric mucin type III (3 g/L, Sigma-Aldrich), and 1,2-dihexadecanoyl-*sn*-glycero-3-phosphocholine (DPPC, 0.5 g/L, Avanti Inc.).³² The mucin concentration of 3 g/L (0.3% w/v) used in this study is widely employed in experimental virology to simulate respiratory fluids. It corresponds to clinically significant mucin levels observed in human respiratory secretions, ranging from 0.1% w/v in healthy individuals to 0.3–0.5% w/v in hypersecretions associated with conditions like smoking, asthma, COPD, and cystic fibrosis.³³ Sodium chloride at 9 g/L (0.9% w/v) replicates the salinity of human bodily fluids, while DPPC at 0.5 g/L mimics the surface-active properties of pulmonary surfactant, essential for droplet stability.³² These formulations approximate the properties of respiratory emissions, enabling realistic assessments of viral stability and inactivation in aerosolized particles under controlled conditions.

After atomization, the particles passed through a homemade coaxial, silica-gel-based diffusion dryer to remove excess humidity and fine water droplets. This was followed by a custom-designed saturator/condenser system for particle growth through condensation (more details about the saturator/condenser system are provided in section S1.1.1 of the Supporting Information). After leaving the saturator/condenser system, the condensate aerosols enter the chamber which is set to a constant temperature (T) of 20 °C and relative humidity (RH) of 55%.

Choice of Virus

T4 phage was employed as target virus to validate the aerosolization system, chamber processes, and sampling step and to evaluate the environmental factors affecting the aerosolized viruses. T4 phage is a virus that infects *Escherichia coli* and is nonpathogenic to humans and animals, ensuring safety and ease of handling under laboratory conditions. T4 phage is a reliable surrogate for baseline data collection for testing concepts to validate the developed experimental setup for future research using pathogenic aerosolized viruses. Future work with pathogenic viruses is required in order to better comprehend aerosol dynamics and various possible deactivation methods.

The phage concentrations in the stock solution ranged from 2.2×10^{10} to 3.7×10^{10} copies/mL, which were diluted to $(4.8\text{--}7.2) \times 10^8$ copies/mL in the atomizer for aerosolization. The concentration of virus in respiratory fluid has been reported to range from 10^5 copies/mL in normal individuals to 10^9 copies/mL for individuals with high viral loads.³⁴ Tseng and Li demonstrated the use of phage concentrations in the nebulizer ranging from 2×10^8 to 7×10^8 titer/mL for aerosolization studies. This range aligns closely with the concentrations we employed, providing further validation for our experimental setup. After aerosolization into the 19 m³ chamber, the airborne viral concentrations were further diluted, mimicking real-world conditions.

Virus Aerosol Chamber ACD-C+V

The Atmospheric Chemistry Department Chamber (ACD-C)^{35–37} was upgraded and then used to perform the experiments of the

present study. This 19 m³ chamber consists of a cylinder with a surface-to-volume ratio of 2 m⁻¹ and is made of Teflon. Reflective aluminum surrounded the chamber, fitted with two light sources: UVA (Cleo Advantage 140W-R XPT) and UVC lamps (UV-Strahler 30W, UMECH GmbH). The UVA lamps were used at two settings: “2-set” with an irradiance of 171.9 W/m² and “3-set” with an irradiance of 475.3 W/m² in the interval of 315 to 400 nm. Additionally, eight UVC lamps, with a peak of 254 nm, were installed around the chamber, providing a total irradiance of 0.36 W/m² (more details about the ACD-C chamber are provided in section S1.1.2 of the Supporting Information).

Sampling of Virus-Laden Particles

To evaluate the effects of light and H₂O₂ on aerosolized viruses, two samplers were selected to collect viruses from the chamber: the SKC BioSampler (20 mL, SKC Inc., Eighty-Four, PA, USA) and the Button aerosol sampler (SKC Inc., Eighty-Four, PA, USA). These samplers are widely recognized for efficiently collecting diverse bioaerosols, including viruses^{38,39} (more details about samplers are presented in section S1.1.4 of the Supporting Information).

Propagation and Titration of Viruses

Propagation of T4 phage was carried out using the liquid broth method with DSM544 medium and *Escherichia coli* (Migula 1895) serving as the host organism. Both T4 phage and *E. coli* were obtained from Deutsche Sammlung von Mikroorganismen und Zellkulturen GmbH (DSMZ, Braunschweig, Germany; more details are provided in section S1.1.5 of the Supporting Information).

Quantification of Phages

Nucleic acids of T4 phage from Biosampler suspensions or dissolved gelatin filters were extracted using the QIAmp Viral RNA Kit (Qiagen, Hilden, Germany) according to the manufacturer's instructions. A sample volume of 550 μL was used. Samples were stored at –20 °C until qPCR was performed. More details are given in section S1.1.6 of the SI.

Quantitative PCR (qPCR) was selected due to its high sensitivity and ability to quantify viral genome copies regardless of viability, making it a robust tool for assessing molecular-level effects of UVC, UVA, and H₂O₂ on aerosolized viruses. While this method highlights molecular damage to the viral genome and provides a proxy for viral inactivation, it may underestimate the true extent of inactivation, as it does not capture other mechanisms such as protein denaturation or envelope disruption. However, prior studies^{31,40,49} demonstrate strong correlations between reductions in genome copy numbers and functional inactivation. Future studies will aim to incorporate advanced techniques such as electron microscopy and molecular assays to directly assess structural changes to viral particles post-treatment, complementing the genome-level analysis presented here.

The evaluation of the qPCR was performed by preparing PCR standards with a known number of genome copies (10^{10} to 10^0). The diagram of PCR number (Ct value) changes corresponding to genome copies is presented in Figure S7 (Supporting Information). The slope of the calibration curve is –3.5198, the y intercept is 41.027, and the factor of determination (R^2) is 0.9947. The PCR efficiency is 92.4% and the limit of detection is 95% at a concentration of 25 genome copies per reaction. By using the qPCR efficient equation, the number of genome copies was calculated as follows:

$$N_{\text{PCR}} = 10^{(\text{Ct} - y - \text{intercept}) / \text{slope}} \quad (1)$$

where N_{PCR} is the number of genome copies detected in the qPCR reaction and Ct is the cycle threshold. To calculate the total number of sampled genome copy equivalents from the chamber (N_{Ch}), it is necessary to consider the dilution from the initial sample taken from the chamber to the volume used for DNA extraction. The N_{Ch} was calculated as follows:

$$N_{\text{Ch}} = \frac{N_{\text{PCR}} V_{\text{S}}}{V_{\text{PCR}} V_{\text{Ali}}} \times V_{\text{Ch}} \quad (2)$$

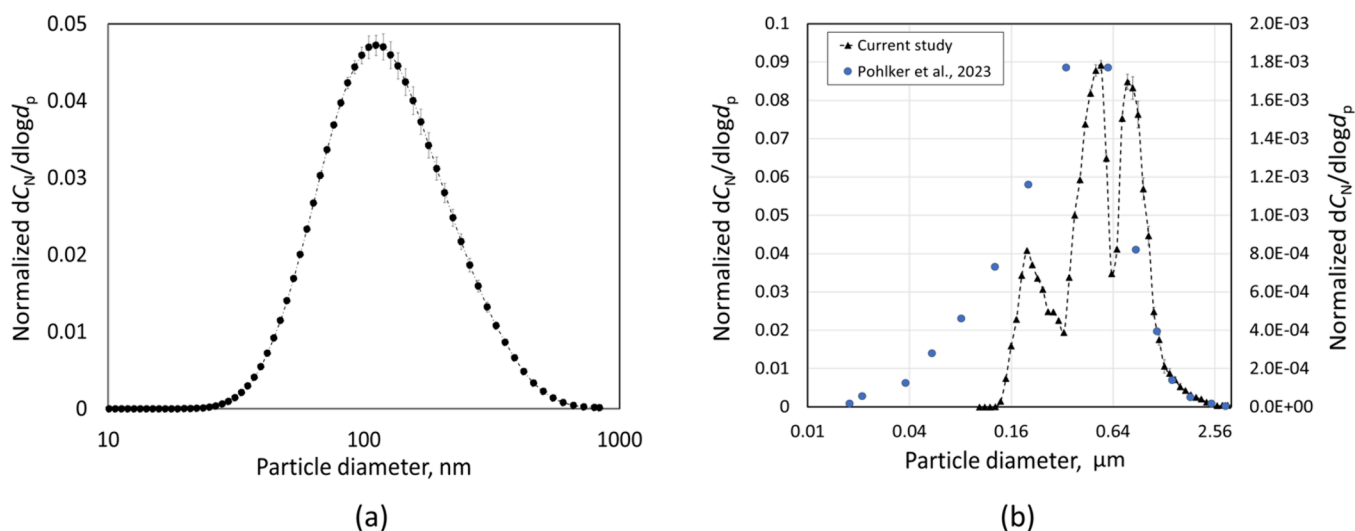


Figure 2. Particle size distribution of ammonium sulfate while the saturator/condenser system is (a) off and (b) on.

V_S is the elution volume of the extraction column, V_{PCR} is the volume used in qPCR, V_{Ali} is the sample volume used to extract DNA, and V_{ch} is the volume of the sampler which was loaded from the chamber.

To better estimate the effect of UVC, UVA, and H_2O_2 on T4 phages, we calculated the detected fraction of genome copy equivalents. The fraction is defined as the ratio of the number of genome copy equivalents detected after exposure to UV light sources, with or without H_2O_2 , to the number detected in the dark condition. The relative fraction of genome copies, $F_{detected}$ is defined as

$$F_{relative} = \frac{N_{Ch_exposed}}{N_{Ch_dark}} \quad (3)$$

Overall Course of Experiment

The experimental process commenced with measuring the size of ammonium sulfate aerosol particles under two conditions: with and without the saturator/condenser system. This comparison was necessary to evaluate the effect of the saturator/condenser system on particle size and, consequently, on virus transportation. To measure the size distribution, after reaching steady-state conditions in the chamber (RH of 55% at 20 °C) and the tube walls and the outlet of the saturator/condenser system, the aerosol particles were introduced into the chamber for 1 h, with the chamber's inlet and outlet kept open to ensure consistent distribution of particles throughout the chamber together with mixing by an internal propeller. After 1 h, the particle injection was stopped, and the chamber was closed and thus changed to batch mode.

In the following, the particle size measurements were conducted every 30 min for 3 h, to assess wall loss and calculate the half-life of aerosolized particles using ammonium sulfate. Particle size distribution was measured by a Scanning Mobility Particle Sizer (SMPS, TROPOS, Germany)^{41,42} when the saturator/condenser system was inactive. All measurements were taken in dark conditions. In order to avoid any changes in particle size due to evaporation, when the saturator/condenser was on, a WELAS 1200 (PALAS, Karlsruhe, Germany) was used. This instrument was designed to keep the aerosol flow in an isothermal and isobaric condition and avoid evaporation.⁴³

To evaluate the effects of the different light sources and H_2O_2 on the viruses, the following procedure was conducted: After steady-state conditions in the chamber were reached (e.g., for temperature and humidity), the process was stopped, and the chamber was changed to the batch mode. Experiments were then continued for a period ranging from 1 to 3 h, depending on the specific experiment, during which various lighting scenarios and the presence or absence of H_2O_2 were tested. details about light sources and H_2O_2 concentrations are presented in sections S1.1.7 and S1.1.8 of the Supporting Information.

As detailed in the Supporting Information (section S1.1.9, Table S2), experiments were conducted with one or two repetitions. Error bars, representing the standard deviation from two independent PCR tests, are included in all of the relevant graphs. For single-repetition experiments, reliability was validated by assessing multiple sampling times (10, 30, and 60 min), with logical trends observed across these intervals (sections S2.2 and S2.3 of the Supporting Information).

RESULTS

Aerosol Particle Size Distribution Measurements

In the deactivated state, the particle size distribution, Figure 2a, displayed a distribution with a mode diameter of 120 nm. The particle distribution is consistent with virus sizes similar to those of SARS-CoV-2,^{44,45} H1N1 influenza,⁴⁶ and T4 phage (with 90 nm head and 200 nm tail).⁴⁷ In contrast, activating the system resulted in a distribution with three peaks at 200, 550, and 850 nm with concentrations of 1.6×10^4 particles/cm³, 3.2×10^4 particles/cm³, and 5.1×10^3 particles/cm³, respectively (Figure 2b). The right vertical axis in Figure 2b represents our current experimental data and the left shows data from Pöhlker et al.,⁴⁸ showing a tidal breathing particle size distribution. This comparison highlights the potential applicability of the experimental setup in replicating real scenarios of respiratory particle emissions.

Total particle wall losses at RH = 55% make approximately 27% reduction in particle number counts after 3 h. The size dependent wall losses for particles of diameters of 850, 550, and 200 nm size are 7%, 15%, and 41%, respectively. The total particle concentration at the start of the measurement was 5.92×10^4 particles/cm³ which reduced to 4.33×10^4 particles/cm³ after 180 min. The higher loss rate of smaller particles can be due to enhanced wall deposition due to the lower Stokes numbers. On the other hand, the possibility that particles with higher Stokes numbers stay airborne for longer times could be due to the circulation of air in the chamber. By using first-order reaction calculations for particle loss over time, we estimated half-lives of approximately 4 h for 200 nm particles and 11 h for 550 nm particles. Further explanation, as well as the size-resolved particle wall loss rate are provided in Figures S8 and S9 and Supporting Information, section S2.1. Additionally, the changes in airborne particle concentrations over time, including a comparison of particle concentrations at $t = 0$

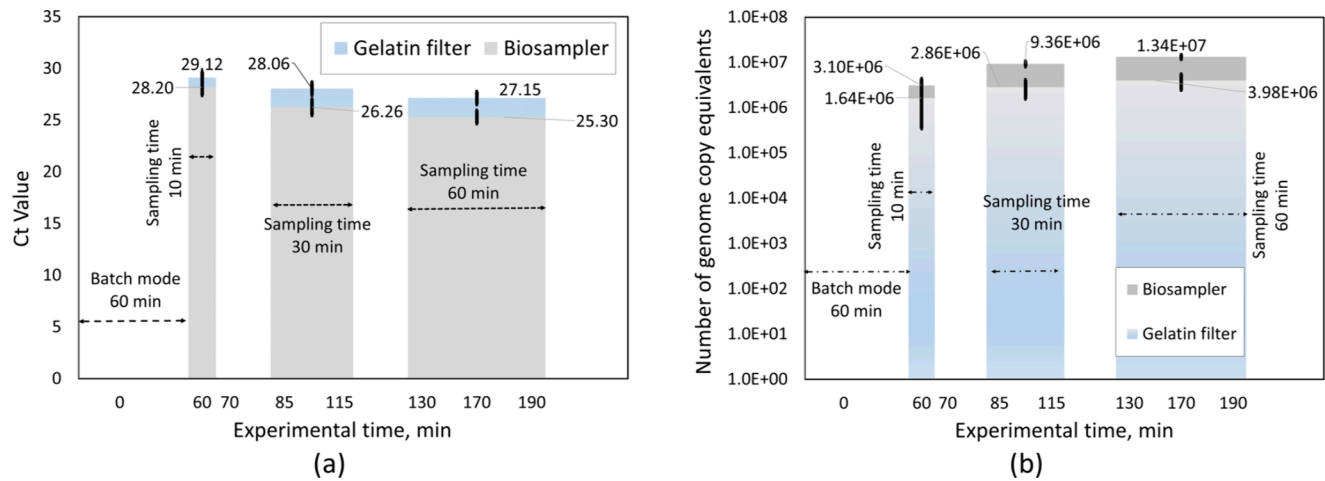


Figure 3. Comparison the T4 phage sampling ability of gelatin filter and SKC BioSampler for different sampling times (a) based on cycle threshold values (Ct) and (b) the number of genome copy equivalents sampled from the chamber.

and $t = 180$ min, are presented in Figure S4 of the Supporting Information.

Comparison of Virus Particle Samplers

To evaluate virus sampling efficiency, two samplers, (A) a gelatin filter and (B) the SKC BioSampler, were tested for their ability to collect T4 phage over sampling durations of 10, 30, and 60 min. The results are shown in Figure 3, which provides a dual perspective based on cycle threshold (Ct) values and the quantified number of genome copy equivalents. A decrease in PCR Ct values from 28.20 to 25.30 was observed for the BioSampler as sampling time increased from 10 to 60 min (Figure 3a). This corresponds to the upward trend of the number of genome copy equivalents (Figure 3b). This number (calculated by eq 2) increased from 3.10×10^6 to 1.34×10^7 by increasing the sampling time from 10 to 60 min, respectively. A similar trend was observed with the gelatin filter; however, it displayed lower sampled genomes copy equivalents (increasing from 1.64×10^6 to 3.98×10^6 as the time went from 10 to 60 min) and consequently higher Ct values, with a smaller reduction observed over time (from 29.12 to 27.15). This observed trend is in line with findings from the literature^{38,39} indicating that for the work performed here, the BioSampler is the better choice than the Button aerosol sampler for sampling the T4 phage from the chamber. In similar investigation, Fabian et al.³⁸ reported that the BioSampler, in comparison with gelatin filters, could yield titers of the infectious influenza virus (H1N1) around an order of magnitude higher. In parallel, Li et al.³⁹ also reported higher Ct values for detection of H1N1 for gelatin filter in comparison with the Biosampler. It is important to note that this finding may originate from various factors, including specific virus types, environmental conditions during sampling, and methodological differences. Based on the results of the comparison, the BioSampler was chosen as the primary sampler for subsequent experiments. Accordingly, all reported Ct values were obtained by using this sampler.

Effects of Chamber Batch Mode Duration

To assess the loss of viral genome copy equivalents due to the wall deposition in the chamber, a series of tests was conducted in dark conditions. In these batch tests an initial virus injection for 1 h was sampled after 1, 2, and 3 h. This series of experiments was designed to evaluate the possible virus

deposition during exposure time on the number of detectable genome copies. Our experimental results showed that the detected genome copies were constant for different batch mode durations, indicating that wall loss had a negligible impact on the number of genome copy equivalents across different time frames (Figure S10, Section S2.2). This baseline characterization demonstrated that the primary factor contributing to the reduction of phage genome copy equivalents within the chamber for experiment times up to 3 h was likely a factor other than particle wall loss such as longer duration of batch experiment, effects of UV radiation, or H₂O₂ addition. Accordingly, batch reactor runs of different duration can be compared with each other as the phage-laden particles mainly stay dispersed or “airborne” during experimental times of 1, 2, and 3 h. Further details related to the UVC dose experiments are provided in Section S2.2 of the Supporting Information.

Virus Loaded in Water vs Mucin in Dark Experiments

To better mimic human exhaled aerosol particles, a deionized water (DI) water-based mixture of porcine gastric mucin plus DPPC and NaCl was used as a medium for the atomizer as well as the first tube of the saturator/condenser system.³² The resulting aerosol was compared with pure DI water in the atomizer as well as the first tube in the dark condition (Figure S12, Section S2.3). The qPCR results indicated that the Ct value increased from 25.3 to 30.43 when mucin was replaced with water. Applying eq 2, this resulted in values of 1.34×10^7 and 1.64×10^5 of genome copy equivalents, respectively. This reduction agreed with the experimental results reported in previous studies by Zuo et al.⁴⁹ and Pan et al.⁵⁰ These studies investigated the effect using various media in the atomizer and reported increasing virus survivability correlated with enhanced mucin concentration. Zuo et al.⁴⁹ explained that the increased survivability can be attributed to the protective barrier of mucin around the virus. This mucin layer shields the virus from deactivating factors by reducing its exposure to environmental stressors, particularly those that can lead to the rearrangement and folding of viral proteins. Woo et al.²³ reported that mucin may shield the virus from deforming mechanical forces, thereby preventing the inactivation of the virus.

The Effect of UVC on Aerosolized Virus

To comprehensively evaluate the effect of UVC irradiation on T4 phages, another set of experiments was conducted. In each

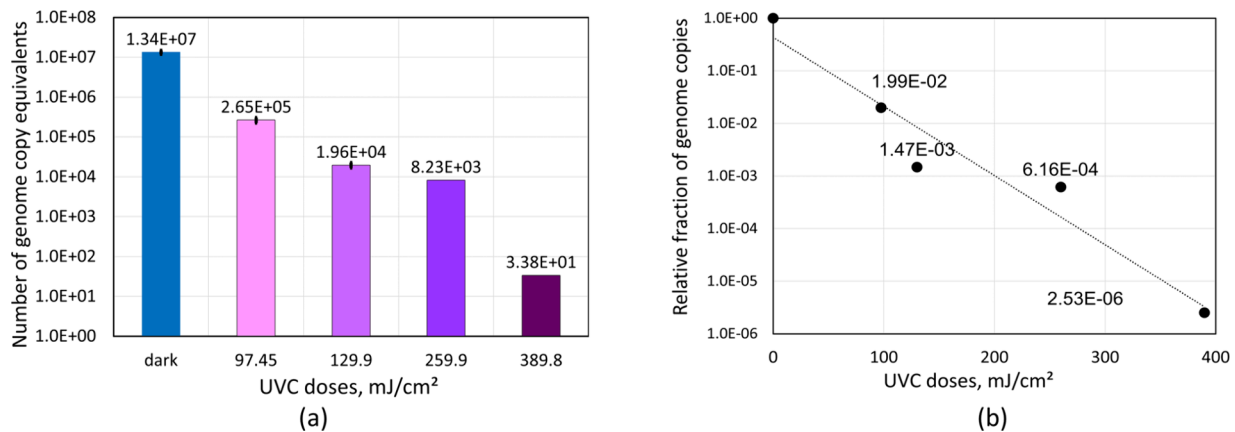


Figure 4. Effect of different UVC doses on aerosolized T4 phage: (a) number of genome copy equivalents sampled from the chamber; (b) relative fraction of genome copies.

experiment, the virus was aerosolized with mucin. Sprayed particles were injected into the chamber for 1 h before switching to batch mode. In this mode, the aerosolized virus particles were subjected to ultraviolet C (UVC) radiation. The dose of UVC received by the virus particles is a function of both the intensity of the UVC light and the duration of exposure. Specifically, the UVC dose can be quantified by the following formula: UVC dose = UVC intensity \times exposure time. This measurement, typically expressed in joules per square meter (J/m^2), indicates the total amount of UVC energy to which the virus particles are exposed over the given period. To assess the effect of UVC doses, the sampled viral load was quantified by measuring genome copy equivalents using qPCR. The findings demonstrated a clear trend between increased UVC doses and a reduction in the detection of the total amount of sampled genome copy equivalents (see Figure 4a). Initially, in the absence of UVC exposure, the number of genome copy equivalents was 1.34×10^7 . Subsequent increases in UVC dosage to 97.45, 129.9, and 259.9 mJ/cm^2 resulted in a decrease in the genome copy equivalents to 2.65×10^5 , 1.96×10^4 , and 8.23×10^3 , respectively. For the UVC doses of 259.9 and 389.8 mJ/cm^2 , the experiments were conducted only once. Despite this limitation, the observed trends were consistent across all sampling times (10, 30, and 60 min), as presented in Section S2.4 and Figures S13 and S15 of the Supporting Information. The alignment of these results with those from multiple-repetition experiments at other UVC doses validates the reliability of the findings.

UVC primarily inactivates viruses by targeting their nucleic acids, forming pyrimidine dimers in DNA or RNA that disrupt the double-helix structure.^{51,52} This genomic damage impairs vital processes such as transcription and replication, effectively halting viral propagation.⁵³ Beyond its effect on genetic material, UVC can also denature key viral proteins essential for host cell entry, replication, or virion assembly.⁵³ In enveloped viruses, UVC compromises structural integrity by damaging surface glycoproteins, further reducing the infectivity.

To better estimate the effect of UVC, the relative fraction of genome copies (calculated by eq 3) for each UVC dose was compared to that in the dark condition (Figure 4b). At integrated UVC dosages of 97.45 mJ/cm^2 (9.2×10^{-3} mW/cm^2 for 3 h), 129.9 mJ/cm^2 (3.61×10^{-3} mW/cm^2 for 1 h), and 259.9 mJ/cm^2 (3.61×10^{-3} mW/cm^2 for 2 h), the relative fraction of genome copies was reduced to 2%, 0.2%, and 0.1%,

respectively, compared to the initial viral load under the dark conditions. These results confirm the efficacy of UVC irradiation for viral inactivation and show that higher doses correlated to larger reductions in detectable viral genome copy equivalents. The efficacy of UVC irradiation was further highlighted at a dose of 389.8 mJ/cm^2 (3.61×10^{-3} mW/cm^2 for 3 h), which resulted in a reduction to 34 genome copy equivalents (estimated 6 order of magnitude reduction compared to the dark condition). The trend of the detected fraction shows an exponential decay as a function of the UVC dose (Figure 4b). The results show that applying a dose of 97.45 mJ/cm^2 reduces the relative fraction to only about 2%. Compared to Tseng and Li's¹⁹ study on other aerosolized bacteriophages, which reported lower necessary doses, our results suggest a higher threshold. Tseng and Li¹⁹ observed effective UVC inactivation already at 2 mJ/cm^2 for *Escherichia* virus MS2 (MS2 phage), *Escherichia* virus ϕ X174 (ϕ X174 phage), *Pseudomonas* phage ϕ 6 (ϕ 6 phage), and *Escherichia* virus T7 (T7 phage). The difference in our findings can be attributed to the mucin as a carrier medium, which increases virus viability in the presence of UVC. Woo et al.²³ reported a similar trend; the inactivation of the MS2 bacteriophage was less pronounced in artificial saliva containing mucin compared to deionized water when exposed to UVC on N95 filters. The results of these authors showed that doubling the UVC dose resulted in an increase of the reduction over 3 orders of magnitude in the case of deionized water, while the effect over artificial saliva, which contains mucin, was found to be less than 1 order of magnitude. Alameddine et al.²⁴ also found that mucin presence reduced UVC disinfection efficacy of aerosolized MS2 on filters. The shielding effect of mucin-containing particles can protect viruses from UVC irradiation.^{23,24} Besides, experiments conducted in a 19 m^3 atmospheric chamber, especially in the batch mode, designed to simulate real-world scenarios, differ significantly from those in Tseng and Li's smaller 0.00055 m^3 semireactor chamber with continuous flow.¹⁹ The larger chamber size introduces greater spatial variability in irradiance, as particles are farther from UV lamps and reflective surfaces and particle movement is more complex. This variability necessitates higher average UVC doses for consistent inactivation compared with the uniform UV exposure achievable in compact chambers. These differences underscore the importance of contextualizing UVC efficacy based on experimental setups and conditions. Further

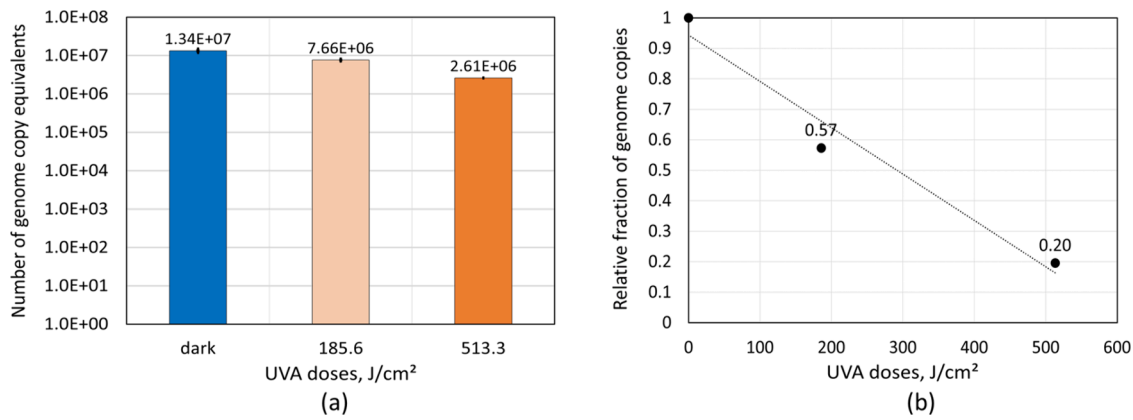


Figure 5. Effect of different UVA doses on aerosolized T4 phage: (a) number of genome copy equivalents sampled from the chamber; (b) relative fraction of genome copies.

details related to the UVC dose experiments are provided in Section S2.4 of the [Supporting Information](#).

The Effect of UVA on Aerosolized Viruses

To evaluate the effect of UVA light on viruses, two doses of 185.60 J/cm² (equivalent to 171.90 W/m² for 3 h) and 513.30 J/cm² (equivalent to 475.30 W/m² for 3 h) were investigated. By exposing the virus to 185.60 J/cm² and 513.30 J/cm², the total number of genome copy equivalents decreased from 1.34 × 10⁷ (under dark conditions representing the baseline) to 7.66 × 10⁶ and 2.61 × 10⁶, respectively (Figure 5a).

The calculations showed that under a dose of 185.60 J/cm², at a temperature of 20 °C and RH of 55%, 44% of the virus was preserved (Figure 5b). Increasing the light dose to 513.30 J/cm² resulted in only 20% preservation of the T4 phage. Comparing these results with those of UVC exposure, it is evident that UVC is much more efficient in reduction of virus genomes. After exposure of the virus to a dose of 97.45 mJ/cm² of UVC, only 2% of the genome copy was detected by qPCR, which is significantly lower than the 513.30 J/cm² of UVA needed to reduce the virus genome copy to 20%. However, the ability of UVA to remove pathogens similar to viruses should also be noted. Our results are in line with previous research by Miyauchi et al.²⁷ and Darnel et al.²⁵ who investigated the effects of UVA and UVC on SARS-CoV-1.

UVA inactivates viruses primarily through indirect mechanisms, generating reactive oxygen species (ROS) that oxidize purine and pyrimidine bases in viral nucleic acids. This oxidative stress can cause single-strand breaks in DNA/RNA, disrupting viral replication.⁵⁴ Additionally, UVA induces lipid peroxidation in viral envelopes, potentially compromising the structural integrity of enveloped viruses.⁵⁵ High doses of UVA can also damage viral proteins, affecting their functionality and ability to bind to host cell receptors.

The Effect of Hydrogen Peroxide on Aerosolized Viruses

To evaluate the effect of hydrogen peroxide (H₂O₂) on the virus, four different concentrations (1.6, 4.0, 8.0, and 16 ppm) were investigated in the absence and presence of UV light sources. The experiments were conducted in the dark as a control and in the presence of light, specifically UVA (185.60 and 513.3 J/cm²) and UVC (97.45 mJ/cm²).

The results in dark conditions showed a continuous decrease in the number of genome copy equivalents from 1.36 × 10⁷ to 3.05 × 10⁶, 1.31 × 10⁶, 9.71 × 10⁵, and 4.66 × 10⁵ for total injected H₂O₂ concentrations of 1.6, 4.0, 8.0, and 16 ppm,

respectively (Figure 6). It is important to note that these figures represent the total amount of hydrogen peroxide

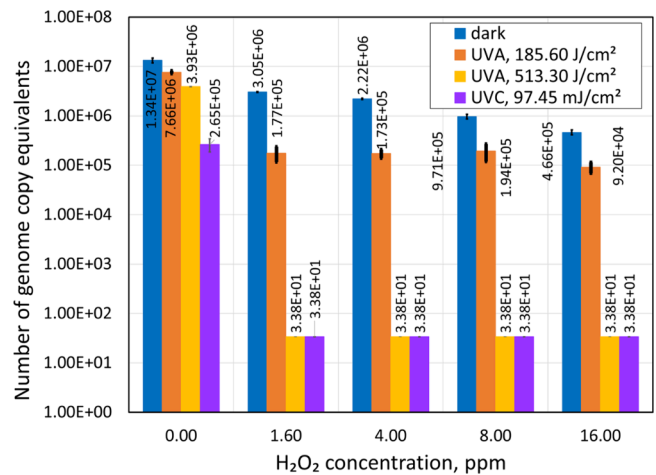


Figure 6. Effect of different H₂O₂ concentrations on T4 phage: number of genome copy equivalents from the chamber.

continuously injected into the chamber over 3 h, during exposure to aerosolized virus in batch mode. The detected fractions were 22%, 10%, 7%, and 3% for these respective concentrations, in the range between 1.6 and 16 ppm added H₂O₂ (Figure 7). Hydrogen peroxide (H₂O₂) inactivates

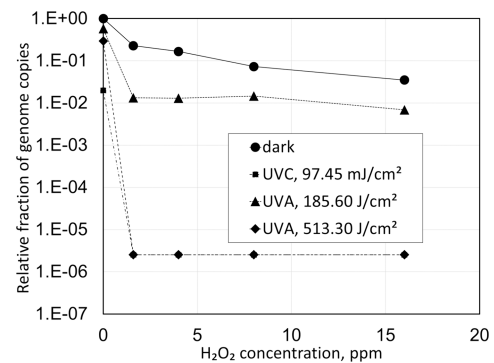


Figure 7. Relative fraction of genome copies of aerosolized T4 phage exposed to different H₂O₂ concentration at RH 55% to dark condition.

viruses through generation of reactive oxygen species (ROS), including hydroxyl radicals ($\bullet\text{OH}$), which play a critical role in disrupting viral envelopes, denaturing proteins, and degrading nucleic acids.^{56,57} These ROS oxidize lipid bilayers in viral envelopes, compromising the structural integrity of enveloped viruses.⁵⁸ Additionally, $\bullet\text{OH}$ induces oxidative modifications in proteins and nucleic acids, leading to loss of functionality and infectivity.⁵⁹

Gomez et al.³¹ reported that a concentration of around 900 ppb hydrogen peroxide injected in 20 s into a 9 m³ chamber at 22 °C and 60% RH, resulted in 50% and 99% inactivation after 6 ± 1 and 38 ± 10 min, respectively, of an airborne murine coronavirus, the mouse hepatitis virus (MHV). The comparison between our results and those of Gomez et al.³¹ indicates that hydrogen peroxide is highly effective for inactivation of viruses, even in the absence of light. The results showed a significant reduction of the detected fraction of genome copy equivalents, up to 78% observed at 1.6 ppm of H₂O₂. When the H₂O₂ concentration was increased to 4.0 ppm, the detected fraction decreased to 10%. Further increasing the H₂O₂ concentration led to a still further reduction in detected genome copy equivalents, although the rate of reduction diminished. Gomez et al.³¹ observed a similar trend, with 50% deactivation occurring in 6 min and requiring about 40 min to deactivate the remaining virus. The comparison implies that high concentrations of hydrogen peroxide, due to the high concentration of reactive oxygen species (ROS), lead to rapid deactivation of virus genome copy equivalents. However, as exposure continues and hydrogen peroxide is consumed, the slope of reduction slows down. Conversely, injecting a lower concentration continuously can achieve the same level of deactivation over a longer period.

The interaction of H₂O₂ with UVA and UVC light to reduce detectable genome copy number equivalents was also investigated. Exposing the phage to 513.30 J/cm² UVA and 97.45 mJ/cm² UVC, alongside H₂O₂, resulted in a reduction of the genome copy equivalents by 6 orders of magnitude, indicating reduction of phage in the number of genome copy equivalents, to 6 orders for all H₂O₂ concentrations studied. Without hydrogen peroxide, the reduction of genome copy equivalents compared to the dark condition was approximately 80% and 90% for UVA and UVC, respectively. Exposing the phage to 185.60 J/cm² UVA in the presence of 1.6 ppm of H₂O₂ decreased the number of genome copy equivalents from 8.0×10^6 to 9.2×10^4 , reducing the detected fraction of viral genomes from 56% to around 1%. Higher concentrations did not significantly alter the detected fraction until 16 ppm, where a notable reduction was observed. The combined use of hydrogen peroxide and UVA significantly decreased the detected fraction of genome copies from 44% to over 99%, which highlights the effectiveness of this disinfection method.

The difference between 185.60 and 513.30 J/cm² in the reduction of the detected virus fraction in the presence of H₂O₂ was attributed to the photon flux associated with each UV dose. While photolysis of H₂O₂ occurred at both doses, the photon flux at 185.60 J/cm² may produce an insufficient amount of hydroxyl radicals ($\bullet\text{OH}$) to overcome scavenging effects by components such as mucin in the carrier medium. These scavenging effects can limit the availability of $\bullet\text{OH}$ radicals to interact directly with the virus. In contrast, the higher UV dose (513.30 J/cm²) provides sufficient photon flux to generate enough $\bullet\text{OH}$ radicals to compensate for scavenging and effectively inactivate the viral genome. At this

dose, additional H₂O₂ concentrations contribute minimally to further inactivation, as the majority of viruses are already inactivated.⁶⁰

A plateau in inactivation efficiency with increasing H₂O₂ concentrations was observed under UV conditions, particularly at 185.60 J/cm². This phenomenon reflects a saturation effect, where additional $\bullet\text{OH}$ radicals generated at higher H₂O₂ concentrations do not significantly enhance disinfection.⁶¹ Excess H₂O₂ may also act as a scavenger for $\bullet\text{OH}$ radicals, forming less reactive species and reducing radical-mediated inactivation efficiency.⁶¹ The sharp initial decline in genome copies under UV exposure, followed by a plateau, contrasts with the gradual, concentration-dependent trend observed in dark conditions, underscoring the critical role of UV intensity in driving H₂O₂ activation.

CONCLUSION

Within the present study, aerosolized T4 phage embedded in mucin were generated in the size range of human respiratory exhalation particles. These particles were injected into an aerosol simulation chamber with a relative humidity of 55% and a temperature of 20 °C to simulate indoor conditions, resembling real-world scenarios. The objective of the study was to investigate the effects of ultraviolet (UV) light and hydrogen peroxide (H₂O₂) on airborne viruses. Our findings show that the mucin in the generated aerosol significantly increases T4 phage's resistance to UVC irradiation, resulting in a 259.9 mJ/cm² dose required for 99.9% genome copy equivalent reduction compared to the 1–2 mJ/cm² reported in previous studies. Besides, in accordance with previous research, our results show that while UVA radiation is less effective than UVC, it is still an option to reduce detected viral genome copy equivalents. At higher doses, such as 513.30 J/cm², UVA was capable of reducing the detected fraction of genome copy equivalents by nearly 80%. The effect of H₂O₂, particularly in combination with UV light, on airborne viruses had not been extensively investigated before. The present study reveals that H₂O₂ can significantly reduce the number of genome copy equivalents, with effectiveness increasing as the concentration rises. For example, at just 1.6 ppm, we observed that 78% of detected genome copy equivalents were reduced compared to the initial condition, which increased to 97% at 16 ppm, even under dark conditions. The combination of H₂O₂ with UV light, particularly UVA, demonstrated remarkable potential to reduce the detected fractions of genome copies by PCR loaded aerosolized viruses. In our experiments, exposure of T4 phage to UVA light, with the dose of 185.60 J/cm², alone achieved only 44% virus genome copy detection compared to the dark condition. However, introducing 1.6 ppm of H₂O₂ boosted the detected fraction to over 99%. Notably, the combination of even low UVC doses or higher UVA doses with hydrogen peroxide concentrations between 1.6 and 16 ppm achieved a 6 order of magnitude reduction of the detected fraction of genome copy equivalents compared to the dark condition.

These results highlight the importance of integrating both chemical and photonic methods in the development of strategies to mitigate airborne viral transmission in various environments. Future research should focus on applying these findings to real human pathogenic viruses to confirm the broader applicability and effectiveness of these methods. The experimental setup, designed to generate virus-laden particles simulating human exhalation, along with the atmospheric chamber, enabled a detailed investigation of the factors

influencing the transmission of aerosolized viruses and the efficacy of various mitigation methods.

■ ASSOCIATED CONTENT

SI Supporting Information

The Supporting Information is available free of charge at <https://pubs.acs.org/doi/10.1021/envhealth.4c00215>.

Additional experimental details; materials and methods, including aerosol generation setup, UV light intensity data, bioaerosol sampling methods, and quantification of virus genomes; Additional experimental results, including the number of repetitions for each experiment and validation (PDF)

■ AUTHOR INFORMATION

Corresponding Author

Hartmut Herrmann – Atmospheric Chemistry Department (ACD), Leibniz Institute for Tropospheric Research (TROPOS), 04318 Leipzig, Germany; orcid.org/0000-0001-7044-2101; Phone: +49-341 235-2446; Email: herrmann@tropos.de; Fax: +49 341 235-2325

Authors

Ali Mohamadi Nasrabadi – Atmospheric Chemistry Department (ACD), Leibniz Institute for Tropospheric Research (TROPOS), 04318 Leipzig, Germany; orcid.org/0009-0003-6091-8542

Diana Eckstein – Department of Technical Biogeochemistry, Helmholtz Centre for Environmental Research (UFZ), 04318 Leipzig, Germany

Peter Mettke – Atmospheric Chemistry Department (ACD), Leibniz Institute for Tropospheric Research (TROPOS), 04318 Leipzig, Germany

Nawras Ghanem – Department of Applied Microbial Ecology, Helmholtz Centre for Environmental Research (UFZ), 04318 Leipzig, Germany

René Kallies – Department of Environmental Microbiology, Helmholtz Centre for Environmental Research (UFZ), 04318 Leipzig, Germany; Federal Environment Agency, Section Microbial Risks, 14195 Berlin, Germany

Matthias Schmidt – Department of Technical Biogeochemistry, Helmholtz Centre for Environmental Research (UFZ), 04318 Leipzig, Germany

Falk Mothes – Atmospheric Chemistry Department (ACD), Leibniz Institute for Tropospheric Research (TROPOS), 04318 Leipzig, Germany; orcid.org/0000-0001-8193-0346

Thomas Schaefer – Atmospheric Chemistry Department (ACD), Leibniz Institute for Tropospheric Research (TROPOS), 04318 Leipzig, Germany; orcid.org/0000-0001-7995-4285

Ricarda Graefe – Atmospheric Chemistry Department (ACD), Leibniz Institute for Tropospheric Research (TROPOS), 04318 Leipzig, Germany

Chaturanga D. Bandara – Department of Technical Biogeochemistry, Helmholtz Centre for Environmental Research (UFZ), 04318 Leipzig, Germany; orcid.org/0000-0002-0688-4260

Melanie Maier – Department of Virology, Institute of Virology, University of Leipzig, D-04103 Leipzig, Germany

Uwe Gerd Liebert – Department of Virology, Institute of Virology, University of Leipzig, D-04103 Leipzig, Germany

Hans Richnow – Department of Technical Biogeochemistry, Helmholtz Centre for Environmental Research (UFZ), 04318 Leipzig, Germany; Isodetect GmbH, 04103 Leipzig, Germany; orcid.org/0000-0002-6144-4129

Complete contact information is available at: <https://pubs.acs.org/doi/10.1021/envhealth.4c00215>

Author Contributions

Ali Mohamadi Nasrabadi: Conceptualization, Experimental setup design and fabrication, Chamber experiments, Writing—original draft. **Diana Eckstein**: qPCR tests, Data analysis, Writing—Materials and Methods section, Writing—review and editing. **Peter Mettke**: Chamber experiments, Writing—review and editing. **Nawras Ghanem**: Provided T4 phages, Writing—review and editing. **René Kallies**: Supervised qPCR tests, Writing—Materials and Methods section, Writing—review and editing. **Matthias Schmidt**: Project discussions, Writing—review and editing. **Falk Mothes**: Initial project planning, Writing—review and editing. **Thomas Schaefer**: Feedback on UV light sources, Writing—review and editing. **Ricarda Graefe**: Experimental setup construction, Chamber experiments. **Chaturanga D. Bandara**: Initial qPCR tests, Writing—review and editing. **Melanie Maier**: qPCR process feedback, Data analysis, Writing—review and editing. **Uwe Gerd Liebert**: Project design and planning, Writing—review and editing. **Hans Richnow**: Project design and planning, Writing—review and editing. **Hartmut Herrmann**: Project conceptualization, Project leadership, Resource provision, Supervision, Writing—review and editing. All authors read and approved the final version of this manuscript.

Notes

The authors declare no competing financial interest.

■ ACKNOWLEDGMENTS

This work was supported by the Federal Ministry of Education and Research (BMBF) under project number 13GW0597E (BeCoLe main project, with subprojects KAPAVIR and MikroVirasol) and the Deutsche Forschungsgemeinschaft (DFG, German Research Foundation) under project number 468717405 (AEROVIR). The authors wish to thank the ProVis Centre for Chemical Microscopy which is supported by European Regional Development Funds (EFRE) and the Helmholtz Association for using its microanalytical facilities. We thank Dr. Rüdiger Hennig (NEL GmbH, Leipzig, Germany) for helping to measure the intensity of UV light sources.

■ REFERENCES

- (1) World Health Organization. COVID-19 Dashboard: Circulating Variants. WHO. <https://data.who.int/dashboards/covid19/circulation?n=0> (accessed Oct 12, 2024).
- (2) Ahmed, H.; Patel, K.; Greenwood, D.; Halpin, S.; Lewthwaite, P.; Salawu, A.; Eyre, L.; Breen, A.; O'Connor, R.; Jones, A.; Sivan, M. Long-term clinical outcomes in survivors of coronavirus outbreaks after hospitalisation or ICU admission: a systematic review and meta-analysis of follow-up studies. *Medrxiv*. 2020.
- (3) Poudel, A. N.; Zhu, S.; Cooper, N.; Roderick, P.; Alwan, N.; Tarrant, C.; Ziauddeen, N.; Yao, G. L. Impact of Covid-19 on health-related quality of life of patients: A structured review. *PLoS one*. 2021, 16 (10), No. e0259164.
- (4) Cutler, D. M.; Summers, L. H. The COVID-19 Pandemic and the \$16 Trillion Virus. *JAMA* 2020, 324 (15), 1495–1496.

- (5) Morawska, L.; Milton, D. K. It Is Time to Address Airborne Transmission of Coronavirus Disease 2019 (COVID-19). *Clin. Infect. Dis.* **2020**, *71*, 2311–2313.
- (6) Morawska, L.; Cao, J. Airborne transmission of SARS-CoV-2: The world should face the reality. *Elsevier Ltd.* **2020**, *139*, No. 105730.
- (7) Van Doremalen, N.; Bushmaker, T.; Morris, D. H.; Holbrook, M. G.; Gamble, A.; Williamson, B. N.; Tamin, A.; Harcourt, J. L.; Thornburg, N. J.; Gerber, S. I.; Lloyd-Smith, J. O.; et al. Aerosol and surface stability of SARS-CoV-2 as compared with SARS-CoV-1. *New Eng. J. Med.* **2020**, *382* (16), 1564–1567.
- (8) Sosnowski, T. R. Inhaled aerosols: Their role in COVID-19 transmission, including biophysical interactions in the lungs. *Curr. Opin. Colloid Interface Sci.* **2021**, *54*, No. 101451.
- (9) National Center for Immunization and Respiratory Diseases (U.S.). Division of Viral Diseases. Scientific Brief: SARS-CoV-2 Transmission. Published May 7, 2021. <https://stacks.cdc.gov/view/cdc/105949> (accessed Oct 12, 2024).
- (10) Mutsch, B.; Heiber, M.; Grätz, F.; Hain, R.; Schönfelder, M.; Kaps, S.; Schraner, D.; Kähler, C. J.; Wackerhage, H. Aerosol particle emission increases exponentially above moderate exercise intensity resulting in superemission during maximal exercise. *Proc. Natl. Acad. Sci. U. S. A.* **2022**, *119* (22), No. e2202521119.
- (11) Zupin, L.; Lichen, S.; Milani, M.; Clemente, L.; Martello, L.; Semeraro, S.; Fontana, F.; Ruscio, M.; Miani, A.; Crovella, S.; Barbieri, P. Evaluation of residual infectivity after SARS-CoV-2 aerosol transmission in a controlled laboratory setting. *Int. J. Environ. Res. Public Health.* **2021**, *18* (21), 11172.
- (12) Berry, G.; Parsons, A.; Morgan, M.; Rickert, J.; Cho, H. A review of methods to reduce the probability of the airborne spread of COVID-19 in ventilation systems and enclosed spaces. *Environ. Res.* **2022**, *203*, No. 111765.
- (13) Hadian, M.; Mazaheri, E.; Jabbari, A. Different approaches to confronting the biological epidemic; prevention tools with an emphasis on COVID-19: A systematized study. *Int. J. Prev. Med.* **2021**, *12* (1), 127.
- (14) Moynihan, R.; Sanders, S.; Michaleff, Z. A.; Scott, A. M.; Clark, J.; To, E. J.; Jones, M.; Kitchener, E.; Fox, M.; Johansson, M.; Lang, E.; et al. Impact of COVID-19 pandemic on utilisation of healthcare services: a systematic review. *BMJ. open* **2021**, *11* (3), No. e045343.
- (15) Reed, N. G. The History of Ultraviolet Germicidal Irradiation for Air Disinfection. *Public Health Rep.* **2010**, *125* (1), 15–27.
- (16) Pereira, A. R.; Braga, D. F.; Vassal, M.; Gomes, I. B.; Simões, M. Ultraviolet C irradiation: A promising approach for the disinfection of public spaces? *Sci. Total Environ.* **2023**, *879*, No. 163007.
- (17) Raeiszadeh, M.; Adeli, B. A critical review on ultraviolet disinfection systems against COVID-19 outbreak: applicability, validation, and safety considerations. *ACS Photonics* **2020**, *7* (11), 2941–2951.
- (18) Heßling, M.; Hönes, K.; Vatter, P.; Lingenfelder, C. Ultraviolet irradiation doses for coronavirus inactivation—review and analysis of coronavirus photoinactivation studies. *GMS Hyg. Infect. Control.* **2020**, *15*, doc08.
- (19) Tseng, C. C.; Li, C. S. Inactivation of virus-containing aerosols by ultraviolet germicidal irradiation. *AS&T.* **2005**, *39* (12), 1136–1142.
- (20) Buonanno, M.; Welch, D.; Shuryak, I.; Brenner, D. J. Far-UVC light (222 nm) efficiently and safely inactivates airborne human coronaviruses. *Sci. Rep.* **2020**, *10* (1), 1–8.
- (21) Walker, C. M.; Ko, G. Effect of Ultraviolet Germicidal Irradiation on Viral Aerosols. *Environ. Sci. Technol.* **2007**, *41*, 5460.
- (22) Derraik, J. G.; Anderson, W. A.; Connelly, E. A.; Anderson, Y. C. Rapid review of SARS-CoV-1 and SARS-CoV-2 viability, susceptibility to treatment, and the disinfection and reuse of PPE, particularly filtering facepiece respirators. *Int. J. Environ. Res. Public Health.* **2020**, *17*, 6117.
- (23) Woo, M. H.; Grippin, A.; Anwar, D.; Smith, T.; Wu, C. Y.; Wander, J. D. Effects of relative humidity and spraying medium on UV decontamination of filters loaded with viral aerosols. *Appl. Environ. Microbiol.* **2012**, *78* (16), 5781–5787.
- (24) Alameddine, M.; Okoro, O.; Wingert, L.; Marchand, G.; Barbeau, B. Impact of the Contamination Method on the Disinfection of N95 Respirators: Drops versus Aerosols. *AAQR.* **2023**, *23* (11), No. 230018.
- (25) Darnell, M. E.; Subbarao, K.; Feinstone, S. M.; Taylor, D. R. Inactivation of the coronavirus that induces severe acute respiratory syndrome, SARS-CoV. *J. Virol. Methods.* **2004**, *121*, 85–91.
- (26) Schuit, M. A.; Larason, T. C.; Krause, M. L.; Green, B. M.; Holland, B. P.; Wood, S. P.; Grantham, S.; Zong, Y.; Zarobila, C. J.; Freeburger, D. L.; Miller, D. M.; et al. SARS-CoV-2 inactivation by ultraviolet radiation and visible light is dependent on wavelength and sample matrix. *J. Photochem. Photobiol., B* **2022**, *233*, No. 112503.
- (27) Miyachi, M.; Sunada, K.; Hashimoto, K. Antiviral effect of visible light-sensitive cuxo/tio2 photocatalyst. *Catalysts* **2020**, *10*, 1093.
- (28) Bono, N.; Ponti, F.; Punta, C.; Candiani, G. Effect of UV irradiation and TiO₂-photocatalysis on airborne bacteria and viruses: An overview. *Materials* **2021**, *14* (5), 1075.
- (29) Toki, T.; Nakamura, K.; Kurauchi, M.; Kanno, T.; Katsuda, Y.; Ikai, H.; Hayashi, E.; Egusa, H.; Sasaki, K.; Niwano, Y. T. Synergistic interaction between wavelength of light and concentration of H₂O₂ in bactericidal activity of photolysis of H₂O₂. *J. Biosci. Bioeng.* **2015**, *119* (3), 358–362.
- (30) Tuladhar, E.; Terpstra, P.; Koopmans, M.; Duizer, E. Virucidal efficacy of hydrogen peroxide vapour disinfection. *J. Hosp. Infect.* **2012**, *80* (2), 110–115.
- (31) Gomez, O.; McCabe, K. M.; Biesiada, E.; Volbers, B.; Kraus, E.; Nieto-Caballero, M.; Hernandez, M. O. Airborne murine coronavirus response to low levels of hypochlorous acid, hydrogen peroxide and glycol vapors. *AS&T.* **2022**, *56* (11), 1047–1057.
- (32) Vejerano, E. P.; Marr, L. C. Physico-chemical characteristics of evaporating respiratory fluid droplets. *J. R. Soc. Interface.* **2018**, *15* (139), No. 20170939.
- (33) Alexander, R. W.; Tian, J.; Haddrell, A. E.; Oswin, H. P.; Neal, E.; Hardy, D. A.; Reid, J. P.; et al. Mucin Transiently Sustains Coronavirus Infectivity through Heterogeneous Changes in Phase Morphology of Evaporating Aerosol. *Viruses* **2022**, *14*, 1856.
- (34) Wang, Y.; Xu, G.; Huang, Y. W. Modeling the Load of SARS-CoV-2 Virus in Human Expelled Particles during Coughing and Speaking. *PLoS One* **2020**, *15*, No. e0241539.
- (35) Zhang, Y.; He, L.; Sun, X.; Ventura, O. N.; Herrmann, H. Theoretical Investigation on the Oligomerization of Methylglyoxal and Glyoxal in Aqueous Atmospheric Aerosol Particles. *ACS. Earth Space Chem.* **2022**, *6* (4), 1031–1043.
- (36) Mettke, P.; Brüggemann, M.; Mutzel, A.; Gräfe, R.; Herrmann, H. Secondary Organic Aerosol (SOA) through Uptake of Isoprene Hydroxy Hydroperoxides (ISOPOOH) and its Oxidation Products. *ACS Earth Space Chem.* **2023**, *7* (5), 1025–1037.
- (37) Mutzel, A.; Rodigast, M.; Iinuma, Y.; Böge, O.; Herrmann, H. Monoterpene SOA—Contribution of first-generation oxidation products to formation and chemical composition. *Atmos. Environ.* **2016**, *130*, 136–144.
- (38) Fabian, P.; McDevitt, J. J.; Houseman, E. A.; Milton, D. K. Airborne influenza virus detection with four aerosol samplers using molecular and infectivity assays: considerations for a new infectious virus aerosol sampler. *Indoor air.* **2009**, *19* (5), 433.
- (39) Li, J.; Leavey, A.; Wang, Y.; O’Neil, C.; Wallace, M. A.; Burnham, C. A. D.; Boon, A. C.; Babcock, H.; Biswas, P. Comparing the performance of 3 bioaerosol samplers for influenza virus. *J. Aerosol Sci.* **2018**, *115*, 133–145.
- (40) Schuit, M. A.; Larason, T. C.; Krause, M. L.; Green, B. M.; Holland, B. P.; Wood, S. P.; Miller, D. M.; et al. SARS-CoV-2 Inactivation by Ultraviolet Radiation and Visible Light Is Dependent on Wavelength and Sample Matrix. *J. Photochem. Photobiol., B* **2022**, *233*, No. 112503.
- (41) Wiedensohler, A.; Birmili, W.; Nowak, A.; Sonntag, A.; Weinhold, K.; Merkel, M.; Wehner, B.; Tuch, T.; Pfeifer, S.; Fiebig, M.; Fjærraa, A. M.; et al. Mobility particle size spectrometers: harmonization of technical standards and data structure to facilitate

high quality long-term observations of atmospheric particle number size distributions. *Atmospheric Measurement Techniques* **2012**, *5* (3), 657–685.

(42) Kroflic, A.; Anders, J.; Drventić, I.; Mettke, P.; Böge, O.; Mutzel, A.; Kleffmann, J.; Herrmann, H. Guaiacol nitration in a simulated atmospheric aerosol with an emphasis on atmospheric nitrophenol formation mechanisms. *ACS Earth Space Chem.* **2021**, *5* (5), 1083–1093.

(43) Jain, M.; Rahatgaonkar, P.; Kandar, T. K.; Ghosh, S.; Chauhan, M. J.; Khan, A. Experimental investigation of CsI aerosol removal in containment spray system test facility of 700 MWe IPHWR. *Nucl. Eng. Des.* **2022**, *390*, No. 111715.

(44) Bar-On, Y. M.; Flamholz, A.; Phillips, R.; Milo, R. SARS-CoV-2 (COVID-19) by the numbers. *Elife*. **2020**, *9*, 57309.

(45) Lee, B. U. Minimum sizes of respiratory particles carrying SARS-CoV-2 and the possibility of aerosol generation. *Int. J. Environ. Res. Public Health*. **2020**, *17* (19), 6960.

(46) Vajda, J.; Weber, D.; Brekel, D.; Hundt, B.; Müller, E. Size distribution analysis of influenza virus particles using size exclusion chromatography. *J. Chromatogr. A* **2016**, *1465*, 117–125.

(47) Xu, J.; Zhao, C.; Chau, Y.; Lee, Y. K. The synergy of chemical immobilization and electrical orientation of T4 bacteriophage on a micro electrochemical sensor for low-level viable bacteria detection via Differential Pulse Voltammetry. *Biosens. Bioelectron.* **2020**, *151*, No. 111914.

(48) Pöhlker, M. L.; Pöhlker, C.; Krüger, O. O.; Förster, J. D.; Berkemeier, T.; Elbert, W.; Fröhlich-Nowoisky, J.; Pöschl, U.; Bagheri, G.; Bodenschatz, E.; Huffman, J. A.; et al. Respiratory aerosols and droplets in the transmission of infectious diseases. *Rev. Mod. Phys.* **2023**, *95* (4), No. 045001.

(49) Zuo, Z.; Kuehn, T. H.; Bekele, A. Z.; Mor, S. K.; Verma, H.; Goyal, S. M.; Raynor, P. C.; Pui, D. Y. Survival of airborne MS2 bacteriophage generated from human saliva, artificial saliva, and cell culture medium. *Appl. Environ. Microbiol.* **2014**, *80* (9), 2796–2803.

(50) Pan, M.; Carol, L.; Lednicky, J. A.; Eiguren-Fernandez, A.; Hering, S.; Fan, Z. H.; Wu, C. Y. Determination of the distribution of infectious viruses in aerosol particles using water-based condensational growth technology and a bacteriophage MS2 model. *AS&T*. **2019**, *53* (5), 583–593.

(51) Garg, H.; Ringe, R. P.; Das, S.; Parkash, S.; Thakur, B.; Delipan, R.; Kumar, A.; et al. UVC-Based Air Disinfection Systems for Rapid Inactivation of SARS-CoV-2 Present in the Air. *Pathogens* **2023**, *12*, 419.

(52) Lo, C. W.; Matsuura, R.; Iimura, K.; Wada, S.; Shinjo, A.; Benno, Y.; Aida, Y.; et al. UVC Disinfects SARS-CoV-2 by Induction of Viral Genome Damage without Apparent Effects on Viral Morphology and Proteins. *Sci. Rep.* **2021**, *11*, No. 13804.

(53) Devitt, G.; Johnson, P. B.; Hanrahan, N.; Lane, S. I.; Vidale, M. C.; Sheth, B.; Mahajan, S.; et al. Mechanisms of SARS-CoV-2 Inactivation Using UVC Laser Radiation. *ACS Photonics* **2024**, *11*, 42–52.

(54) Sadraei, M.; Zhang, L.; Aavani, F.; Biazar, E.; Jin, D. Viral Inactivation by Light. *Light* **2022**, *2*, 18.

(55) Zhao, Y.; Dong, J. Effect of Inactivating RNA Viruses by Coupled UVC and UVA LEDs Evaluated by a Viral Surrogate Commonly Used as a Genetic Vector. *Biomed. Opt. Express* **2022**, *13*, 4429–4444.

(56) Dembinski, J. L.; Hungnes, O.; Hauge, A. G.; Kristoffersen, A. C.; Haneberg, B.; Mjaaland, S. Hydrogen Peroxide Inactivation of Influenza Virus Preserves Antigenic Structure and Immunogenicity. *J. Virol. Methods* **2014**, *207*, 232–237.

(57) Amanna, I. J.; Raué, H. P.; Slifka, M. K. Development of a New Hydrogen Peroxide-Based Vaccine Platform. *Nat. Med.* **2012**, *18*, 974–979.

(58) Urushidani, M.; Kawayoshi, A.; Kotaki, T.; Saeki, K.; Mori, Y.; Kameoka, M. Inactivation of SARS-CoV-2 and Influenza A Virus by Dry Fogging Hypochlorous Acid Solution and Hydrogen Peroxide Solution. *PLoS One* **2022**, *17*, No. e0261802.

(59) Bounty, S.; Rodriguez, R. A.; Linden, K. G. Inactivation of Adenovirus Using Low-Dose UV/H₂O₂ Advanced Oxidation. *Water Res.* **2012**, *46*, 6273–6278.

(60) Sherchan, S. P.; Snyder, S. A.; Gerba, C. P.; Pepper, I. L. Inactivation of MS2 Coliphage by UV and Hydrogen Peroxide: Comparison by Cultural and Molecular Methodologies. *J. Environ. Sci. Health A* **2014**, *49*, 397–403.

(61) Ng, T. W.; An, T.; Li, G.; Ho, W. K.; Yip, H. Y.; Zhao, H.; Wong, P. K. The Role and Synergistic Effect of the Light Irradiation and H₂O₂ in Photocatalytic Inactivation of Escherichia coli. *J. Photochem. Photobiol. B Biol.* **2015**, *149*, 164–171.